Visible Light Induced Photoelectrochemical Properties of n-BiVO4 and n-BiVO4/pCo3O4

ARTICLE *in* THE JOURNAL OF PHYSICAL CHEMISTRY C · JANUARY 2008

Impact Factor: 4.77 · DOI: 10.1021/jp075605x

3 AUTHORS, INCLUDING:

Mingce Long
Shanghai Jiao Tong University
52 PUBLICATIONS **1,630** CITATIONS
SEE PROFILE

Horst Kisch
Friedrich-Alexander-University of Erlangen-N…
256 PUBLICATIONS **6,976** CITATIONS
SEE PROFILE

Visible Light Induced Photoelectrochemical Properties of n-$BiVO_4$ and n-$BiVO_4$/p-Co_3O_4

Mingce Long,[†,‡] Weimin Cai,[†] and Horst Kisch*[,‡]

School of Environment Science and Engineering, Shanghai Jiao Tong University, 800 Dong Chuan Road, Shanghai 200240, People's Republic of China, and Institute of Inorganic Chemistry, University of Erlangen-Nürnberg, Egerlandstrasse 1, Erlangen D-91058, Germany

Received: July 17, 2007; In Final Form: October 17, 2007

The visible light induced photoelectrochemical properties of the pressed powder electrodes n-$BiVO_4$, p-Co_3O_4, and n-$BiVO_4$/p-Co_3O_4 containing 0.8 wt % cobalt were investigated. At pH 7 flatband potentials of −0.30 and +0.54 V vs NHE were measured for the bismuth vanadate and cobalt oxide, respectively, whereas −0.31 V was obtained for $BiVO_4$/Co_3O_4. At a bias of 0.1 V vs Ag/AgCl the n-type photocurrent of $BiVO_4$ changes to p-type upon prolonged irradiation, whereas it remains n-type at the much higher bias of 1.0 V vs Ag/AgCl. The change in conductivity type can be rationalized by invoking oxidation of water to a surface peroxide species. From the photocurrent decay of $BiVO_4$ under chopped irradiation the presence of efficient charge recombination is indicated. It can be suppressed by addition of iodide, thiocyanate, or methanol, leading to about twice as large incident-photon-to-current efficiencies (IPCE). Different from that, in the case of the $BiVO_4$/Co_3O_4 electrode the IPCE values do not change in the presence of iodide or thiocyanate and are 4 times higher. This distinct difference is rationalized by the assumption that the photogenerated charges are efficiently separated at the $BiVO_4$−Co_3O_4 interface forming a type of n-/p-junction. Whereas electrons migrate to the n-type component, holes move to the p-type material. In summary, modification of n-$BiVO_4$ by p-Co_3O_4 stabilizes the photocurrent, increases the efficiency of its generation, and leads to a compartmentalization of interfacial reduction and oxidation at the n-type component and p-type component, respectively.

1. Introduction

Photoactive nanocrystalline semiconductors have been employed in numerous systems such as water splitting,[1,2] detoxification,[3] organic synthesis,[4] dye sensitized solar cells,[5] and light-driven logical gates.[6,7] Application of electrochemical techniques enables in situ investigation of interfacial electron transfer and modulation of the rate-limiting step of a photocatalytic process.[8] Photoelectrochemical experiments allow estimation of the band gap,[9] band edge positions,[10] and details of charge transfer.[11]

Although wide band gap semiconductors such as TiO_2 and ZnO have been investigated extensively, they are in general not photocatalytic when excited by visible light, which is a basic requirement for efficient solar energy utilization. Therefore, other oxidic materials capable of photoinduced charge separation upon excitation in the visible spectral region have gained new interest. An example is $BiVO_4$, which exhibits good photoelectrochemical[12,13] properties and also catalytic activity in photooxidations[14−16] when irradiated at $\lambda \leq 520$ nm (∼2.4 eV). However, when prepared by solution or solid-state methods, $BiVO_4$ always displays low activity, most likely due to its low specific surface of about 0.7 m^2/g.[17] Kohtani et al. reported surface modification with silver accelerated photooxidation reactions.[18,19] Further investigations revealed that a silver loaded $BiVO_4$ film exhibited an about 2 times higher photocurrent.[13] Designing multicomponent nanojunction photocatalysts is an important strategy to enhance the photocatalytic performace.[20−22] However, little attention has been paid to the photoelectrochemistry of n-/p-type composites.

Recently we found that an n-$BiVO_4$/p-Co_3O_4 composite powder containing 0.8 wt % cobalt exhibited significantly enhanced photocatalytic activity in phenol degradation.[17] This material has a specific surface area of about 1.4 m^2/g and consists of micrometer-size bismuth oxide covered by 20−50 nm cobalt oxide particles. In the diffuse reflectance spectrum the presence of Co_3O_4 is clearly evidenced by the weak maximum at about 740 nm corresponding to a transition from the valence band to a localized cobalt(III) sub-band gap state (Figure 1).[23,24] The steep absorption onset at 520 nm arises primarily from the band-to-band absorption of bismuth vanadate (520 nm) and to a lesser extent to that of Co_3O_4, which starts at 604 nm.[23,24] Surprisingly, n-$BiVO_4$/p-Co_3O_4 turned out to be about 16 times more active in phenol photooxidation than unmodified bismuth oxide.[17] On the basis of calculated band edge positions and the fact that the presence of cobalt oxide leads to complete quenching of the bismuth vanadate luminescence, it was rationalized that improved charge separation at the n/p interface is responsible for the activity increase. In the present paper photoelectrochemical experiments on the components and on the composite, in the form of pressed powder electrodes on conducting glass, were performed to gain further insight into the mechanism of charge separation and charge localization.

2. Experimental Section

2.1. Preparation of Electrodes. The yellow $BiVO_4$ powders were prepared in aqueous medium as reported by Kohtani et al.[16] Black Co_3O_4 powder was synthesized by precipitating $Co(NO_3)_2$ solution with $NH_3 \cdot H_2O$, and then separating the precipitate and calcining in air at 500 °C for 10 h. The presence of the Co_3O_4 crystal phase has been established by X-ray diffrac-

* Corresponding author. Fax: +49- 9131-8527363. E-mail: horst.kisch@chemie.uni-erlangen.de.
† Shanghai Jiao Tong University.
‡ University of Erlangen-Nürnberg.

10.1021/jp075605x CCC: $40.75
Published on Web 12/22/2007

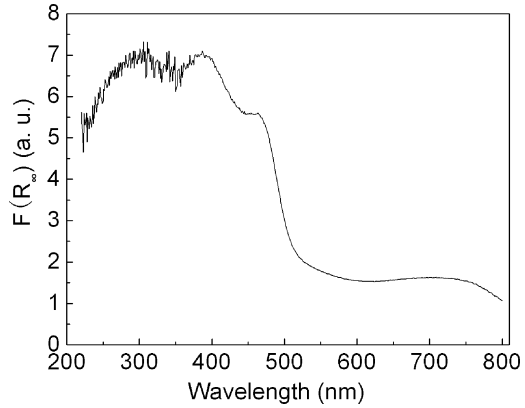

Figure 1. Diffuse reflectance spectrum of the $BiVO_4/Co_3O_4$ composite.

tion (XRD) and its low photocatalytic activity has been established by phenol oxidation, exhibiting less than 4% degradation in 180 min of irradiation time (for details, see ref 17). The preparation of $BiVO_4/Co_3O_4$ composites (if not specified, the sample cobalt content is 0.8 wt %) was performed by impregnation of bismuth vanadate with cobalt(II) nitrate and calcination at 300 °C for 2 h as described previously.[17] Diffuse reflectance spectra were obtained on a Shimadzu UV-2401PC UV/vis scanning spectrophotometer equipped with a diffuse reflectance accessory, and the reflectance was converted by the instrument software to $F(R_\infty)$ values according to the Kubelka−Munk method.

The working electrodes were prepared on indium tin oxide (ITO) glass plates (Praezision Glas & Optik, Iserlohn, Germany, sheet resistance of ~10 Ω/square). The ITO glass pieces with a size of 2.5 × 1.5 cm were sonicated in acetone and degreased in boiling NaOH (0.1 M), and then rinsed with deionized water and dried in an air stream. A suspension of 200 mg of the powder in 1 mL of absolute ethanol was used for casting onto the ITO glass substrate, whose side part was previously protected using Scotch tape. The coated glasses covered with another clean glass slide were pressed under a pressure of 200 kg/cm^2 (IR pressing tool, Paul Weber, Stuttgart, Germany), and then heated at 400 °C in air for 2 h to improve adhesion. A copper wire was connected to the side part of the ITO glass using a conductive tape to establish an ohmic contact. Uncoated parts of the electrodes were isolated with parafilms, and the exposed area of the electrodes under illumination was 0.636 cm^2.

2.2. Photoelectrochemical Experiments. Flatband potential measurements were carried out on an optical train by irradiation with the full light of an XBO 150 W lamp. An 80 mg sample of powder and 10 mg of $(MV)Cl_2$ (methylviologen dichloride, Fluka) or $(DP)Br_2$ (4,5-dihydro-3*a*,5*a*-diazapyrene dibromide, prepared according to ref 25) were suspended in a 100 mL three-necked flask with 50 mL of 0.1 M KNO_3. A platinum plate and a saturated calomel electrode (SCE) served as working and reference electrodes, respectively. Suspensions were magnetically stirred and flushed with N_2 during the measurement. The pH value was adjusted with HNO_3 and N_2 purged NaOH solutions and monitored with a pH meter. Flatband potentials and band edge positions apply for pH 7 and are given relative to normal hydrogen electrode (NHE).

The photoelectrochemical setup consisted of three parts: a tunable monochromatic light source provided with a 1000 W xenon lamp and a universal grating monochromator Multimode 4 (AMKO, Tornesch, Germany), a BAS Epsilon Electrochemistry potentiostat (BAS, West Lafayette, IN), and a three-electrode setup with a platinum plate and a Ag/AgCl electrode (0.207 V vs NHE) serving as the counter and reference electrodes, respectively. Photocurrent measurements were carried out in a Na_2SO_4 (0.5 M) electrolyte, which was purged with nitrogen for 10 min prior to the measurements, but nitrogen was supplied only to the gas phase above the electrolyte during the experiments. The working electrodes were irradiated from the back side (substrate/semiconductor interface) in order to minimize the influence of thickness of the semiconductor layer. The current−potential curves of the Co_3O_4 electrode were obtained in NaOH (0.1 M; pH 12.7) in the dark or illuminated with the full light of a 200 W Hg−Xe arc lamp (Spectral Energy, Model LH-150) at a potential sweep rate of 5 mV/s. The dependence of photocurrent on applied potential for $BiVO_4$ and $BiVO_4/Co_3O_4$ composite was measured under monochromatic light (420 nm) chopped with light and dark phases of 5 s at a sweep rate of 5 mV/s. The wavelength dependence of photocurrent was measured at a constant potential using the chopped monochromatic light with 10 nm bandwidth. The value of photocurrent density was taken as the difference between current density under irradiation and in the dark. The incident-photon-to-current efficiency (IPCE) for each wavelength was calculated according to eq 1:

$$\text{IPCE (\%)} = \frac{i_{ph} hc}{\lambda P e} \times 100 \qquad (1)$$

wherein i_{ph} is the photocurrent density, h is Planck's constant, c is the velocity of light, λ is the irradiation wavelength, e is the elementary charge, and P is the light power density. The spectral dependence of the lamp power density was measured by the optical power meter Oriel 70260 (Oriel, Stratford, CT).

2.3. Estimation of Co(II) Turnover. The total mass of Co_3O_4 per electrode can be estimated as follows. From the concentration of the suspension one obtains that one drop (as applied to the electrode of 1 cm^2) contains about 5 mg of the composite. Recalling that the photoactive area of the electrode is 0.636 cm^2, the content of cobalt is 0.8%, and only one-third of it is due to Co(II), one arrives at a value of about 1×10^{-7} mol of Co(II) present in one electrode. The number of photogenerated holes is estimated from the from the photocurrent density of about 60 μA/cm^2 at 420 nm illumination. Then after 1 h of irradiation about 0.137 μA was produced per electrode surface. This corresponds to about 1×10^{-6} mol of holes, i.e., 10 times more than necessary for the complete reduction of Co(II). Since the electrode was stable for at least 10 h of irradiation several days of irradiation, it seems very unlikely that the photogenerated holes oxidize the metal ion but rather water oxidizes to a surface peroxide species.

3. Results and Discussion

3.1. Flatband Potentials of n-$BiVO_4$ and p-Co_3O_4. The flatband potential of a semiconductor is a property of basic importance for the thermodynamics of the interfacial electron transfer steps occurring in photocatalysis. However, whereas many new materials were reported in the literature exhibiting photocatalytic activity, only in a few cases the position of the flatband potential has been measured. It can be determined by photoelectrochemical methods of photocurrent onset and open circuit potential[9,26,27] and the slurry method,[28] by the electrochemical Mott−Schottky method,[27,29] and by spectroelectrochemistry.[30−32] In the case of $BiVO_4$ Sayama et al. have reported a value of −0.60 V vs Ag/AgCl by the Mott−Schottky method.[13] In this work we obtained the flatband potential by measuring the quasi-Fermi level of electrons by the slurry method.[28] For a heavily doped n-type semiconductor it can be

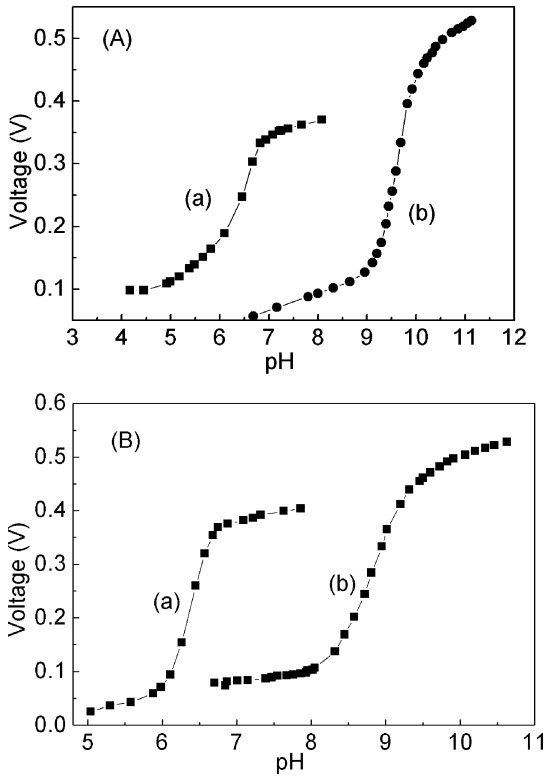

Figure 2. Photovoltage vs suspension pH value measured for (A) $BiVO_4$ and (B) $BiVO_4/Co_3O_4$ in 0.1 M KNO_3 in the presence of (a) DP^{2+} and (b) MV^{2+}. A 100 W XBO lamp, full light.

assumed that the positions of the flatband potential and quasi-Fermi level are the same. The method is based on the pH dependence of the photovoltage in the presence of a pH-independent redox couple such as methylviologen (MV^{2+}, $E°$ = −0.45 V) or the diazaphenanthrene derivative DP^{2+} ($E°$ = −0.27 V). The inflection point (pH_0) of the experimentally obtained voltage vs pH curve is located at 9.60 pH units in the case of MV^{2+} (Figure 2A). The flatband potential at any pH can be calculated according to eq 2:

$$E_{fb}(\mathrm{pH}) = E° - k(\mathrm{pH} - \mathrm{pH}_0) \quad (2)$$

wherein $E°$ is the standard reduction potential of the redox couple. To obtain the value of k, which for oxidic single-crystal semiconductors in general is about 0.059 V/pH,[33] pH_0 may be measured in the presence of at least two different redox couples.[34,35] In this work DP^{2+} was selected as another redox system, affording for $BiVO_4$ a pH_0 value of 6.32. Applying eq 3[33] a k-value of 0.054/pH is calculated, from which the flatband

$$k = (E°_{MV^{2+/+}} - E°_{DP^{2+/+}})/(pH_{0(DP^{2+})} - pH_{0(MV^{2+})}) \quad (3)$$

potential at pH 7 is obtained according to eq 2 as −0.30 V vs NHE. Adding the band gap energy of 2.4 eV results in a valence band edge position of 2.1 V.

Co_3O_4 is a p-type semiconductor with a small band gap of 2.07 eV,[36] and basic photoelectrochemical properties such as the flatband potential are not known in the literature. Attempts to obtain it via the slurry method failed, probably due to the very low photocatalytic activity of this black metal oxide as evidenced in phenol degradation (see Experimental Section). However, the flatband potential can also be estimated from the photocurrent onset.[26,37] The cathodic photocurrent increases with increasing cathodic potential, establishing the p-type semiconductor behavior of Co_3O_4. Photogenerated holes are transferred

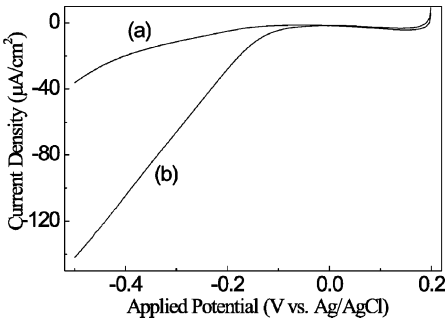

Figure 3. Current−potential plots for Co_3O_4 in NaOH solution (pH 12.7): (a) dark; (b) illuminated by the full light of a 200 W Hg−Xe arc lamp.

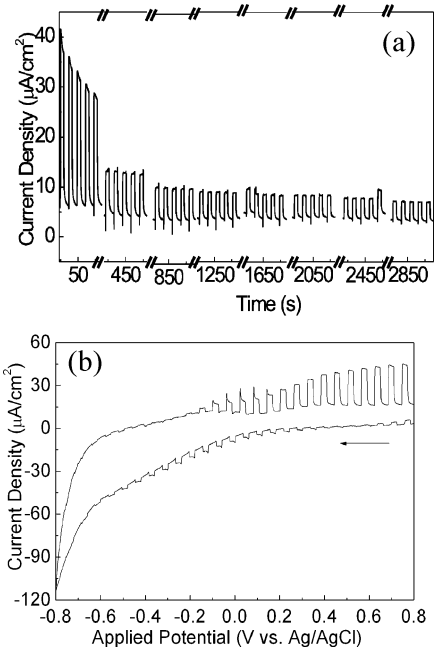

Figure 4. (a) Photocurrent time dependence of $BiVO_4$ upon chopped irradiation with 420 nm light; 0.5 M Na_2SO_4, 1.0 V vs Ag/AgCl. (b) Cyclic voltammogram after 3000 s of irradiation at 420 nm (scan rate of 5 mV/s); arrows indicate start direction of sweep potential.

to the conducting glass substrate producing the cathodic photocurrent. At the present stage of this investigation it cannot be decided if the photogenerated electrons reduce water, traces of oxygen still present in the electrolyte, or even Co(III). From the onset potential of about +0.0 V vs Ag/AgCl at NaOH (Figure 3) electrolyte, a flatband potential of +0.54 V vs NHE at pH 7 is obtained assuming a k-value of 59 mV/pH unit. With the band gap energy of 2.07 eV, the conduction band edge position is calculated as −1.53 V vs NHE.

Different from the failure of Co_3O_4 to afford a significant photovoltage signal in the slurry method, this was the case for the $BiVO_4/Co_3O_4$ electrode exhibiting a pH dependence almost identical to that of bismuth vanadate (Figure 2B). From the pH_0 values of 6.36 and 8.85 obtained in the presence of DP^{2+} and MV^{2+}, respectively, an average quasi-Fermi level of electrons of −0.31 V is calculated assuming a k-value of 59 mV/pH unit. This does not significantly differ from the value of −0.30 V measured for bismuth vanadate and therefore indicates that the reduction of the dipyridinium acceptors takes place at the n-type bismuth vanadate component.

3.2. Stability of $BiVO_4$ and $BiVO_4/Co_3O_4$ Electrodes. Since a crucial point of a photoelectrochemical device is electrode stability, the time dependence of the photocurrent was studied

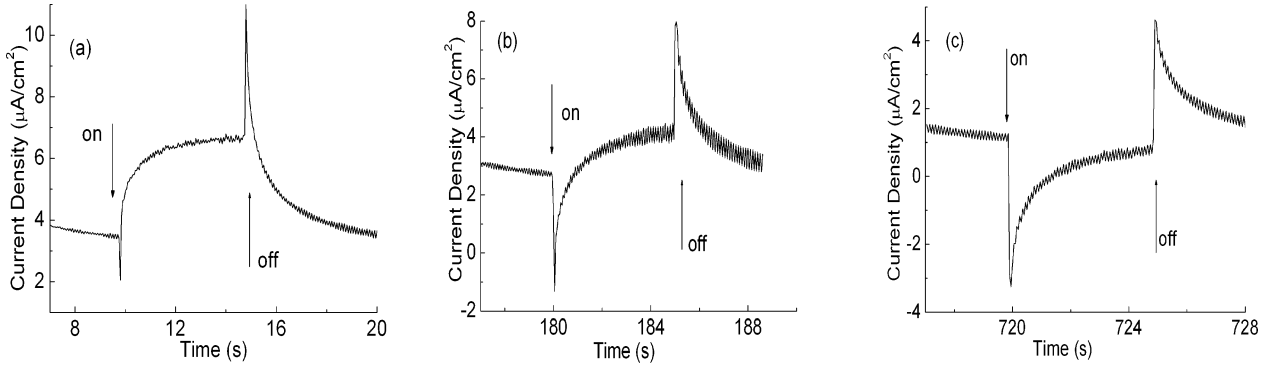

Figure 5. Photocurrent transients of $BiVO_4$ observed after (a) 10, (b) 180, and (c) 720 s of chopped irradiation at 420 nm; 0.5 M Na_2SO_4, 0.10 V vs Ag/AgCl.

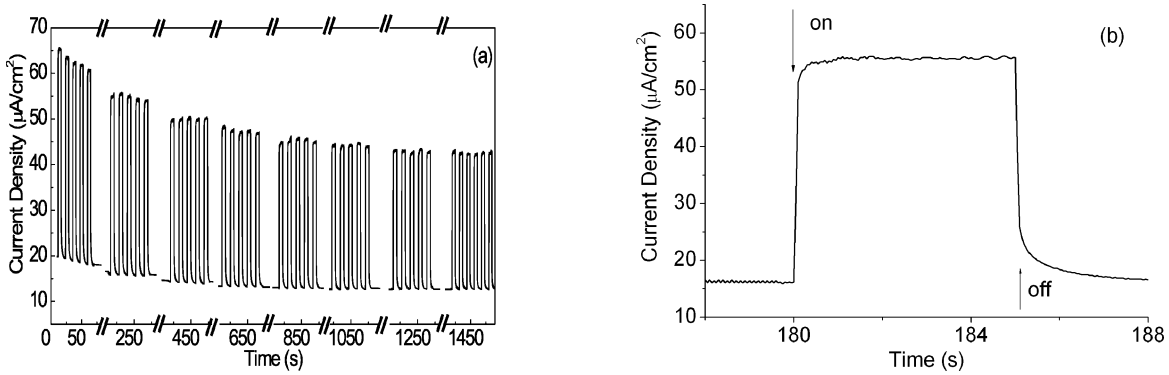

Figure 6. Photocurrent time dependence of $BiVO_4$ in 0.1 M KI upon chopped irradiation with 420 nm light; 0.5 M Na_2SO_4. (a) Time dependence, 0.5 V vs Ag/AgCl. (b) Transient behavior after 180 s of irradiation, 0.5 V vs Ag/AgCl (see also Figure 5b).

in both the absence and presence of iodide as a hole scavenger. In the case of $BiVO_4$ in the absence of iodide the anodic photocurrent decreased by 70% within the first 300 s and then much more slowly (Figure 4a). As recently reported,[13] the photocurrent could be restored by more than 80% through cyclic voltammetry starting with the cathodic scan (Figure 4b). This suggests that during irradiation a surface peroxo species is formed via hole oxidation of water as also reported for titania electrodes,[38] which in the voltammetric or dark experiment is reduced back to water, restoring the original surface. These surface species most likely are the recombination centers responsible for the strong initial photocurrent decrease. More information on the nature of the recombination processes was obtained when the photocurrent was monitored at a low applied bias within the irradiation interval of 5 s in dependence of increasing overall irradiation time (Figure 5). After 10 s a cathodic spike was observed simultaneously with switching on the light, followed by its fast decrease and rise of an anodic current. An anodic overshoot appeared concomitantly with turning off the light (Figure 5a). A similar charging−discharging character has been observed on Prussian Blue surface modified TiO_2.[39,40] Upon further chopped irradiation, the cathodic spike increased whereas the anodic current decreased (Figure 5b). After 720 s irradiation time the anodic current has disappeared whereas the cathodic current and anodic overshoot were still present. This behavior suggests that at the low anodic bias of 0.1 V vs Ag/AgCl the $BiVO_4$ electrode changes its character from n-type to p-type (Figure 5). Since for metal oxide semiconductors the n-type character is generally assumed to arise from oxygen vacancies,[41] it seems likely that formation of the surface peroxo species results in a decrease of oxygen vacancies. The peroxo species may scavenge photogenerated electrons and thus promote hole transfer to the ITO contact, resulting in a cathodic photocurrent. Different from that, no change in photocurrent direction is observable when the bias is as high as 1.0 V vs Ag/AgCl (Figure 4). A similar observation was reported by Jing et al. for n-ZnO, which transformed into a p-type material upon prolonged irradiation as evidenced by surface photovoltage measurements.[42]

To support the conclusions made above, further photocurrent measurements were performed in the presence of 0.1 M potassium iodide as a hole scavenger, assuming that it may inhibit formation of surface peroxo species and therefore stabilize the photocurrent. As shown in Figure 6a, the photocurrent within the first 300 s indeed decreased only by 15% and remained constant thereafter. Furthermore, the transient shape strongly differs from that observed in the absence of iodide (Figure 5b), suggesting the absence of efficient recombination and the presence of a fast oxidation of iodide by the photogenerated hole (Figure 6b).

Modifying the surface of n-$BiVO_4$ with 0.8 wt % cobalt affords the n-/p-composite $BiVO_4$/Co_3O_4. This electrode after 300 s of chopped irradiation suffered a decrease of 30% (Figure 7a). No decrease was observable when the amount of cobalt was increased to 6.4 wt % (Figure 7b). However, since the sample containing the lower cobalt content exhibited a much higher photocatalytic activity in the photooxidation of phenol,[17] this sample was employed in all further experiments.

3.3. Photoelectrochemical Properties of Electrodes. Figure 8 shows the cyclic voltammograms during 420 nm excitation of $BiVO_4$ and the standard $BiVO_4$/Co_3O_4 composite containing 0.8 wt % cobalt. For bismuth vanadate the increasing anodic photocurrent with increasing positive potential indicates n-type semiconductor behavior: electrons migrate to the ITO contact and holes oxidize water. It is known that water cleavage into hydrogen and oxygen under visible light is possible at $BiVO_4$ slurries or electrodes.[13,43] The curves exhibit distinct differences upon changing the potential sweep direction. In the case of a

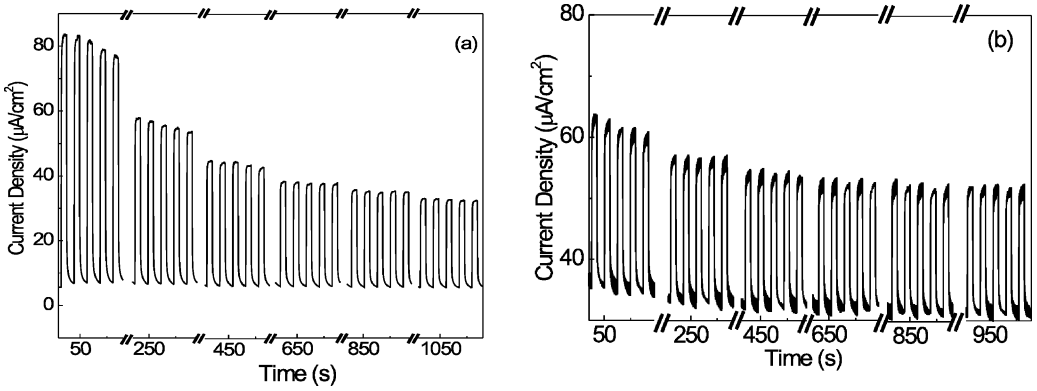

Figure 7. Photocurrent time dependence of $BiVO_4/Co_3O_4$ upon chopped irradiation with 420 nm light; 0.5 M Na_2SO_4, 1.0 V vs Ag/AgCl: (a) 0.8 wt % Co (standard composite); (b) 6.4 wt % Co.

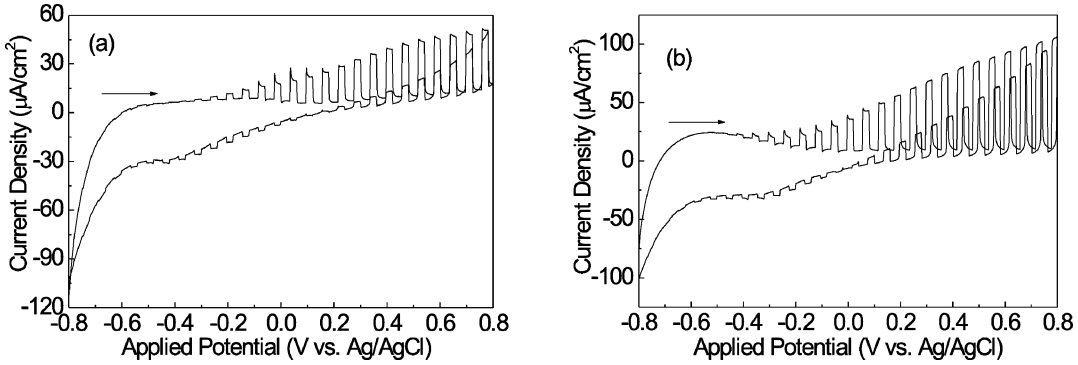

Figure 8. Cyclic voltammograms of (a) $BiVO_4$ and (b) $BiVO_4/Co_3O_4$ electrodes in 0.5 M Na_2SO_4 upon chopped irradiation with 420 nm light. Scan rate of 5 mV/s, 1.0 V vs Ag/AgCl); arrows indicate the start direction of potential sweep.

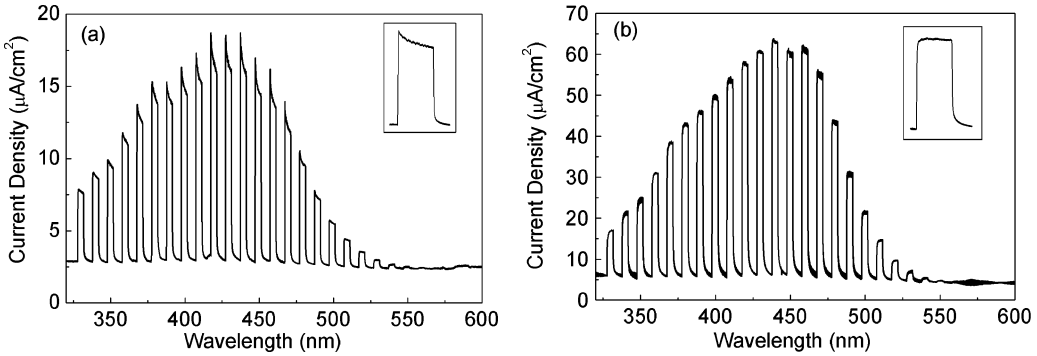

Figure 9. Photocurrent action spectra of (a) $BiVO_4$ and (b) $BiVO_4/Co_3O_4$ under chopped irradiation; 0.5 M Na_2SO_4, 1.0 V vs Ag/AgCl. Insets: photocurrent transients at $\lambda = 420$ nm.

negative-to-positive sweep, the onset potential of the anodic photocurrent of $BiVO_4$ was about −0.40 V vs Ag/AgCl at pH 5.80 (Figure 8a), which is close to the flatband potential of −0.44 V vs Ag/AgCl as calculated for this pH value from the value obtained with the slurry method (vide supra). Upon reversing the potential from the positive to negative direction, the anodic photocurrent became much lower than in the forward sweep, gradually decreased, and turned to a weak cathodic photocurrent at about +0.1 V vs Ag/AgCl. This resembles the photocurrent transient behavior observed with increasing irradiation times (see Figure 5) and can be rationalized as above through formation of surface peroxo species[38] or the effect of adsorbed O_2,[44] both serving as electron scavengers and inducing therefore a p-type behavior. At increasingly negative potentials adsorbed oxygen or peroxo intermediates may be completely reduced, and therefore no more cathodic photocurrent can be generated. The composite electrode afforded very similar results. As already observed by the slurry method (Figure 2), the onset potential of the anodic photocurrent of about −0.42 V vs Ag/AgCl does not differ significantly from that of −0.40 V measured for $BiVO_4$. However, the photocurrent at an applied potential of 0.8 V vs Ag/AgCl is about 2 times higher. This higher efficiency of current generation parallels the photocatalytic activity. In the degradation of phenol this photoelectrochemcial diode is about 16 times more active than $BiVO_4$.[17]

To further investigate the effect of Co_3O_4 loading, the photocurrent action spectra have been measured (Figure 9). Both for $BiVO_4$ and the composite the current extends up to 550 nm, which corresponds to the absorption edge of $BiVO_4$. Apparently Co_3O_4 loading does not shift the photocurrent to longer wavelengths, although Co_3O_4 absorbs up to 855 nm. Different from that, a significant influence of the cobalt component was observed in the photocurrent transients (Figure 9, insets). The initial anodic photocurrent spike and its subsequent decay as observed for bismuth vanadate is a typical indication of surface recombination (vide supra).[9,45,46] This significant recombination even under relatively high bias can be attributed to large particle size[17] and oxygen vacancies.[41] For the $BiVO_4/Co_3O_4$ composite,

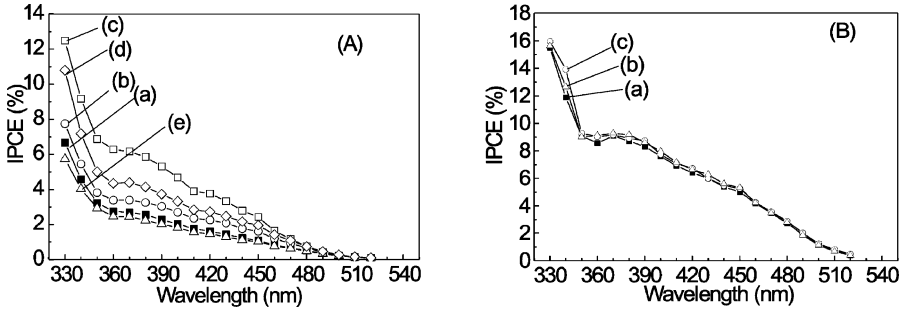

Figure 10. Dependence of the "incident-photon-to-current efficiency" (IPCE) on wavelength for (A) $BiVO_4$ and (B) $BiVO_4$/Co_3O_4 electrodes in 0.5 M Na_2SO_4, +1.0 V vs Ag/AgCl. (a) Without additives; in the presence of (b) methanol (10 vol %), (c) KI (1.25 mM), (d) KSCN (1.25 mM), and (e) KBr (1.25 mM).

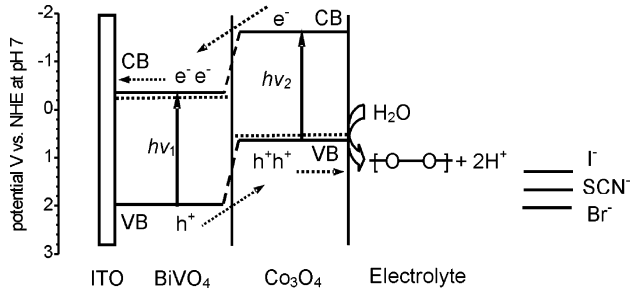

Figure 11. Simplified scheme of the primary processes occurring upon visible light excitation of an n-$BiVO_4$/p-Co_3O_4 electrode. Note that the figure does not represent a layer-by-layer structure. Values of $h\nu_1$ and $h\nu_2$ correspond to 520 and 604 nm, respectively.

no anodic photocurrent spike was observable, thus indicating that the presence of Co_3O_4 inhibits charge recombination.

To obtain further information on the influence of the cobalt component on the efficiency of charge generation, the wavelength dependence of the "incident-photon-to-current efficiency" (IPCE) was studied (Figure 10). Whereas for both electrodes the IPCE value in a similar way quite strongly decreases upon excitation at longer wavelengths and exhibits a distinct shoulder at about 360 nm, distinct differences are found in the presence of various hole scavengers. For $BiVO_4$ the rather low IPCE value of 1.5% at 420 nm increases by factors of 1.4, 1.7, and 2.5 when methanol, thiocyanate, and iodide are present, respectively (Figure 10A). This sequence parallels the increasing reducing power of the additive, suggesting that charge recombination is partially suppressed by fast hole oxidation of these substrates. Only bromide does not follow the correlation, since it has no significant influence, suggesting that the oxidation potential of the reactive hole is less positive than 2.0 V vs NHE, the standard potential of $Br^{\bullet}/Br^{-}$. This compares well with the position of the valence band obtained as about 2.1 V vs NHE (vide supra). The result on the addition of KSCN differs from the previous report,[47] according to which enhancement was observable only under UV excitation whereas a decrease occurred at visible excitation. This difference suggests a slightly more positive location of the valence band edge in the present materials.

For $BiVO_4$/Co_3O_4 the IPCE value at 420 nm is about 4 times larger (Figure 10B). Surprisingly, addition of a hole scavenger did not significantly alter this value. This suggests that the reactive hole is not able to oxidize these additives more efficiently than water. This distinct difference can be rationalized by considering the energetic situation in an idealized scheme assuming the presence of an n-/p-heterojunction (Figure 11). Upon irradiation at wavelengths between 330 and 520 nm both the $BiVO_4$ and Co_3O_4 components generate electron−hole pairs, which mainly localize at $BiVO_4$ due to the large excess of this component. Whereas the electrons are able to move easily to the ITO contact, the holes are expected to migrate in the opposite direction toward the cobalt oxide part. If they are trapped at the bismuth component, the presence of a reducing agent should increase the photocurrent, but that was never observed. This agrees with the fact that the flatband potentials of $BiVO_4$ and $BiVO_4$/Co_3O_4 are almost the same (vide supra). Accordingly, the holes are trapped at the Co_3O_4 component at a potential not positive enough to oxidize methanol or iodide. This is a surprising result, suggesting that water oxidation to a surface peroxo species is more efficient. An alternative oxidation of Co(II) is very unlikely since the photocurrent remained constant through prolonged irradiation, indicating no substantial change in the Co(II) concentration (see Experimental Section). It is noted that cobalt oxide electrodes are known as a catalyst in the electrochemical oxidation of water to oxygen.[2,48−52]

4. Conclusions

The results presented above demonstrate that loading bismuth vanadate with cobalt(II,III) oxide improves the efficiency of photoinudced charge separation. According to the experimentally derived band edge positions, an n-/p-type heterojunction is formed. Upon excitation of this composite, electrons move to bismuth vanadate and holes to the cobalt oxide. Since the valence band edge of the latter is less positive than the potential required for iodide oxidation, the presence of this reducing agent does not influence the efficiency of photon-to-current conversion. Opposite that, in the case of the unmodified bismuth oxide the valence band edge is more positive and iodide increases the efficiency by a factor of about 2.5.

Acknowledgment. We thank Dr. Radim Beranek for stimulating discussions. Financial support by the Specialized Research Fund for the Doctoral Program of Higher Education (SRFDP, 20050248015), from the China Ministry of Education, by the Shanghai Tongji Gao Ting-yao Environmental Science & Technology Development Foundation, and by Deutsche Forschungsgemeinschaft is greatly acknowledged.

References and Notes

(1) Kudo, A. *Int. J. Hydrogen Energy* **2006**, *31*, 197−202.
(2) Kay, A.; Cesar, I.; Graetzel, M. *J. Am. Chem. Soc.* **2006**, *128*, 15714−15721.
(3) Hoffmann, M. R.; Martin, S. T.; Choi, W. Y.; Bahnemann, D. W. *Chem. Rev.* **1995**, *95*, 69−96.
(4) Kisch, H. *Adv. Photochem.* **2001**, *26*, 93−144.
(5) Graetzel, M. *Nature* **2001**, *414*, 338−344.
(6) Furtado, L. F. O.; Alexiou, A. D. P.; Goncalves, L.; Toma, H. E.; Araki, K. *Angew. Chem., Int. Ed.* **2006**, *45*, 3143−3146.
(7) Szaciłowski, K.; Macyk, W.; Stochel, G. *J. Am. Chem. Soc.* **2006**, *128*, 4550−4551.
(8) Jiang, D. L.; Zhang, S. Q.; Zhao, H. J. *Environ. Sci. Technol.* **2007**, *41*, 303−308.
(9) Beranek, R.; Kisch, H. *Electrochem. Commun.* **2007**, *9*, 761−766.

(10) Nakamura, R.; Tanaka, T.; Nakato, Y. *J. Phys. Chem. B* **2004**, *108*, 10617−10620.
(11) Beranek, R.; Neumann, B.; Sakthivel, S.; Janczarek, M.; Dittrich, T.; Tributsch, H.; Kisch, H. *Chem. Phys.* **2007**, http://dx.doi.org/10.1016/j.chemphys.2007.05.022.
(12) Sayama, K.; Nomura, A.; Zou, Z. G.; Abe, R.; Abe, Y.; Arakawa, H. *Chem. Commun.* **2003**, 2908−2909.
(13) Sayama, K.; Nomura, A.; Arai, T.; Sugita, T.; Abe, R.; Yanagida, M.; Oi, T.; Iwasaki, Y.; Abe, Y.; Sugihara, H. *J. Phys. Chem. B* **2006**, *110*, 11352−11360.
(14) Zhou, L.; Wang, W. Z.; Liu, S. W.; Zhang, L. S.; Xu, H. L.; Zhu, W. *J. Mol. Catal. A* **2006**, *252*, 120−124.
(15) Zhang, L.; Chen, D. R.; Jiao, X. L. *J. Phys. Chem. B* **2006**, *110*, 2668−2673.
(16) Kohtani, S.; Makino, S.; Kudo, A.; Tokumura, K.; Ishigaki, Y.; Matsunaga, T.; Nikaido, O.; Hayakawa, K.; Nakagaki, R. *Chem. Lett.* **2002**, *31*, 660−661.
(17) Long, M. C.; Cai, W. M.; Cai, J.; Zhou, B. X.; Chai, X. Y.; Wu, Y. H. *J. Phys. Chem. B* **2006**, *110*, 20211−20216.
(18) Kohtani, S.; Hiro, J.; Yamamoto, N.; Kudo, A.; Tokumura, K.; Nakagaki, R. *Catal. Commun.* **2005**, *6*, 185−189.
(19) Kohtani, S.; Tomohiro, M.; Tokumura, K.; Nakagaki, R. *Appl. Catal., B* **2005**, *58*, 265−272.
(20) Long, M. C.; Cai, J.; Cai, W. M.; Chen, H.; Chai, X. Y. *Prog. Chem.* **2006**, *18*, 1065−1075.
(21) Kim, H. G.; Borse, P. H.; Choi, W.; Lee, J. S. *Angew. Chem., Int. Ed.* **2005**, *44*, 4585−4589.
(22) Tada, H.; Mitsul, T.; Kiyonaga, T.; Akita, T.; Tanaka, K. *Nat. Mater.* **2006**, *5*, 782−786.
(23) Cheng, C. S.; Serizawa, M.; Sakata, H.; Hirayama, T. *Mater. Chem. Phys.* **1998**, *53*, 225−230.
(24) Barreca, D.; Massignan, C.; Daolio, S.; Fabrizio, M.; Piccirillo, C.; Armelao, L.; Tondello, E. *Chem. Mater.* **2001**, *13*, 588−593.
(25) Huenig, S.; Gross, J.; Lier, E. F.; Quast, H. *Liebigs Ann. Chem.* **1973**, 339−358.
(26) Pleskov, Yu. V.; Mazin, V. M.; Evstefeeva, Yu. E.; Varnin, V. P.; Teremetskaya, I. G.; Laptev, V. A. *Electrochem. Solid-State Lett.* **2000**, *3*, 141−143.
(27) Khan, S. U. M.; Akikusa, J. *J. Phys. Chem. B* **1999**, *103*, 7184−7189.
(28) Roy, A. M.; De, G. C.; Sasmal, N.; Bhattacharyya, S. S. *Int. J. Hydrogen Energy* **1995**, *20*, 627−630.
(29) Bolts, J. M.; Wrighton, M. S. *J. Phys. Chem.* **1976**, *80*, 2641−2645.
(30) Boschloo, G.; Fitzmaurice, D. *J. Phys. Chem. B* **1999**, *103*, 2228−2231.
(31) O'Regan, B.; Graetzel, M.; Fitzmaurice, D. *Chem. Phys. Lett.* **1991**, *183*, 89−93.
(32) Rusina, O.; Macyk, W.; Kisch, H. *J. Phys. Chem. B* **2005**, *109*, 10858−10862.
(33) Morrison, S. R. *Electrochemistry at semiconductor and oxidized metal electrodes*; Plenum Press: New York, 1980; p 154.
(34) Macyk, W.; Burgeth, G.; Kisch, H. *Photochem. Photobiol. Sci.* **2003**, *2*, 322−328.
(35) Kisch, H.; Burgeth, G.; Macyk, W. *Adv. Inorg. Chem.* **2004**, *56*, 241−259.
(36) Gulino, A.; Fragala, I. *Inorg. Chim. Acta* **2005**, *358*, 4466−4472.
(37) Trari, M.; Bouguelia, A.; Bessekhouad, Y. *Sol. Energy Mater. Sol. Cells* **2006**, *90*, 190−202.
(38) Ulmann, M.; de Tacconi, N. R.; Augustynski, J. *J. Phys. Chem.* **1986**, *90*, 6523−6530.
(39) Szaciłowski, K.; Macyk, W.; Stochel, G. *J. Mater. Chem.* **2006**, *16*, 4603−4611.
(40) Hebda, M.; Stochel, G.; Szaciłowski, K.; Macyk, W. *J. Phys. Chem. B* **2006**, *110*, 15275−15283.
(41) Vinke, I. C.; Diepgrond, J.; Boukamp, B. A.; de Vries, K. J.; Burggraaf, A. J. *Solid State Ionics* **1992**, *57*, 83−89.
(42) Jing, L. Q.; Xin, B. F.; Yuan, F. L.; Wang, B. Q.; Shi, K. Y.; Cai, W. M.; Fu, H. G. *Appl. Catal., A* **2004**, *275*, 49−54.
(43) Kudo, A.; Omori, K.; Kato, H. *J. Am. Chem. Soc.* **1999**, *121*, 11459−11467.
(44) Neumann, B.; Bogdanoff, P.; Tributsch, H.; Sakthivel, S.; Kisch, H. *J. Phys. Chem. B* **2005**, *109*, 16579−16586.
(45) Qian, X. M.; Qin, D. Q.; Song, Q.; Bai, Y. B.; Li, T. J.; Tang, X. Y.; Wang, E. K.; Dong, S. J. *Thin Solid Films* **2001**, *385*, 152−161.
(46) Peter, L. M. *Chem. Rev.* **1990**, *90*, 753−769.
(47) Liu, H. M.; Nakamura, R.; Nakato, Y. *J. Electrochem. Soc.* **2005**, *152*, G856−G861.
(48) Bocca, C.; Cerisola, G.; Magnone, E.; Barbucci, A. *Int. J. Hydrogen Energy* **1999**, *24*, 699−707.
(49) Svegl, F.; Orel, B.; Grabec-Svegl, I.; Kaucic, V. *Electrochim. Acta* **2000**, *45*, 4359−4371.
(50) Brunschwig, B. S.; Chou, M. H.; Creutz, Q.; Ghosh, P.; Sutin, N. *J. Am. Chem. Soc.* **1983**, *105*, 4832−4833.
(51) Behl, W. K.; Toni, J. E. *J. Electroanal. Chem.* **1971**, *31*, 63−75.
(52) Elizarova, G. L.; Zhidomirov, G. M.; Parmon, V. N. *Catal. Today* **2000**, *58*, 71−88.